

HFEMI Data From Carbon Rods, Wires, and Improvised Explosive Device Constituent Parts

Benjamin E. Barrowes^a, Danney Glaser^a, Mikheil Prishvin^b, Guy Jutras^c, Kevin O'Neill^b, and Fridon Shubitidze^b.

^aUS Army Engineer Research and Development Center, 72 Lyme Rd., Hanover, NH 03755

^bThayer School of Engineering, Dartmouth College, Hanover NH 03755

^cGeophex, Ltd., 605 Mercury street, Raleigh NC 27603

ABSTRACT

High-frequency electromagnetic induction (HFEMI) extends the established EMI frequency range above 100 kHz to perhaps 20 MHz. In this higher frequency range, less-conductive targets display heretofore unseen responses in their inphase and quadrature components. Improvised explosive device constituent parts, such as carbon rods, small pressure plates, conductivity voids, low metal content mines, and short wires respond to HFEMI but not to traditional EMI. Results from recent testing over mock-ups of less conductive IEDs or their components show distinctive HFEMI responses, suggesting that this new sensing realm could augment the detection and discrimination capability of established EMI technology. The electrical conductivity of soil may contribute, in effect, to the imaginary part of the permittivity of soil and may then, in turn, generate perceptible responses in traditional EMI. In HFEMI, both the real and complete imaginary parts of soil permittivity produce notable effects. Pursuing this, lab tests with tap water and variously saturated Ottawa sand were compared with results from time domain reflectometry.

Keywords: electromagnetic induction, landmine detection, high frequency EMI, voids, IED

1. INTRODUCTION

Electromagnetic wave theory offers the potential for acquiring information about discrete targets and bulk media even when those targets are obscured or buried. In order to acquire information through soils, with typical conductivities in the range of 0.001 to 0.1 siemens per meter, appropriately low frequencies must be chosen in order to minimize losses related to the skin effect.¹ Ground penetrating radar, typically utilizing frequencies from 100 MHz to 3 GHz, suffers from the rapid attenuation of its transmitted fields, but with the benefit of having a short enough wavelength to guide the radiation in a preferred direction.²⁻⁴ Electromagnetic induction, on the other hand, suffers from the inability to direct the radiation due to the long wavelengths and from the low resolution imposed by low frequencies. It is also limited by... a rapid decay in the transmitted fields of $1/r^3$ from the first term of the Hertzian dipole, but has the advantage of being able to treat the soil as if it were transparent in most cases.^{1,5-9} EMI has performed well, for example, in recent land-based detection and discrimination tests for finding metallic targets such as UXO in the near subsurface (i.e. ≈ 1 meter).¹⁰⁻¹²

High-frequency electromagnetic induction (HFEMI) operates in between these two frequency extremes. Loosely defined as the frequency regime from 100 kHz to 20 MHz, HFEMI produces long enough wavelengths to still satisfy magneto-quasistatic assumptions. And previously unavailable data in the secondary field from responses by less conducting targets, voids, and short wires all have demonstrated the promise of operating in this frequency regime. With the increased frequency, we encountered difficulties with wavelength coherency and noise associated with resonance that we have detailed elsewhere.¹³⁻¹⁵ After overcoming these challenges, we have fabricated three types of high-frequency electromagnetic induction sensors using different coil configurations to buck the primary field in the receiver coils (see Figure 1). With these sensors, we have been able to detect emerging carbon fiber shell unexploded ordnance (UXO) on military ranges¹⁰⁻¹² as well as evidence of depleted uranium both in solid and dispersed forms.^{16,17}

With these higher frequencies, we have also been able to detect less conducting targets that are typically found as constituent parts of improvised explosive devices.¹⁸⁻²¹ For example, carbon rods are often extracted from batteries and

Further author information:

E-mail: benjamin.e.barrowes@erdc.dren.mil, Telephone: +1 (603)646-4822

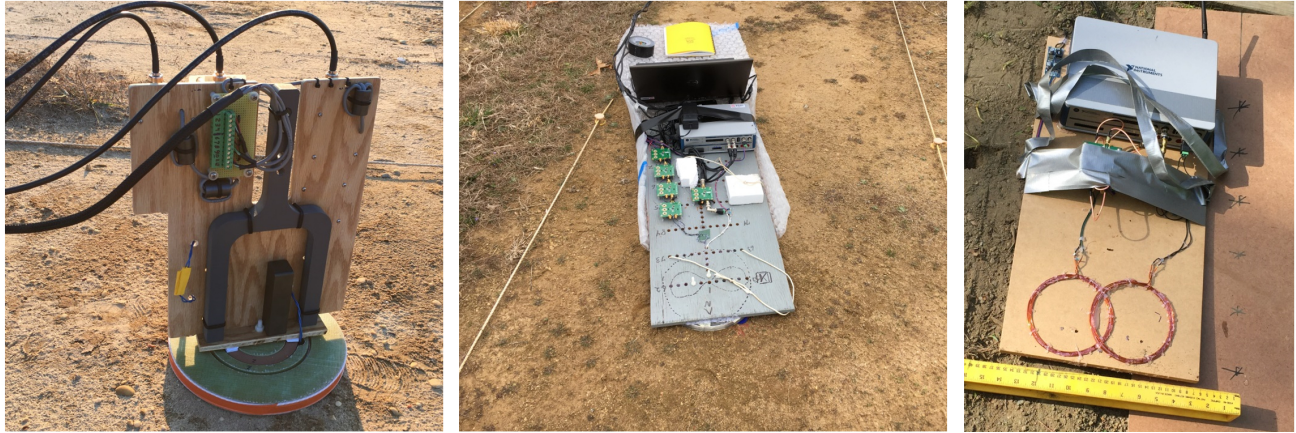


Figure 1: Three different variants of the HFEMI sensor: (Left) Geophex GEM-3 type with concentric transmitter and receiver coils. (Center) figure 8 quadruple receiver type. (Right) overlapping coil type.

used to complete the circuit of the primitive pressure switches in these devices.²² The conductivity of these carbon rods is typically on the order of thousands of siemens per meter, whereas most metals have conductivity in the millions of siemens per meter. As a result, these carbon rods are only detectable along with their broadband signature at frequencies above 100 kHz.^{13,14,23} In addition, because the relaxation spectrum in the inphase and quadrature components of the response from metal targets shifts to higher frequencies the smaller the metal target is, the small metal pins in low metal content landmines are also detectable at HFEMI frequencies.^{6,18}

When detecting and classifying subsurface targets using electromagnetic induction, the response from the soil is usually a nuisance and must be subtracted or modeled out. This must be done at HFEMI frequencies as well, but rather than a nuisance, the large soil response possible at these higher frequencies enables extra information to be acquired from bulk media that was not available at lower EMI frequencies. While soil conductivity has been interrogated for several decades using frequencies as low as 300 Hz,²⁴ extracting soil permittivity from induction frequencies is only now becoming possible in this HFEMI band as we bridge the gap between traditional EMI and radar frequencies. As predicted by Labson and others,^{25–27} we see the evidence of permittivity effects in the low megahertz regime which we are now using to fabricate a standoff permittivity sensor which could for example be mounted on a unmanned aerial system.

The organization of the remainder of this paper is as follows, Section 2 will present electromagnetic induction theory along with special considerations for high-frequency electromagnetic induction. Section 3 will present results from our field test of the HFEMI sensor in all three configurations at the Fort AP Hill IED test lanes. Section 4 will show results from acquiring HFEMI data for soil at Yuma proving grounds as well as for tapwater with a known conductivity, and finally for Ottawa sand at varying levels of water saturation. This is followed by a conclusion.

2. EMI PHENOMENOLOGY

According to Lenz's law, a conducting object in a primary alternating magnetic field will develop eddy currents to oppose the changing flux inside the object^{28,29} with these eddy currents depending on the conductivity of the object. In turn, these eddy currents produce a secondary alternating magnetic field that is out of phase with the primary field. In metals, conductivity and electron mobility is high, which allows induced opposing currents to form (again via Lenz's law) at lower frequencies than in lower-conducting materials. In other words, the time rate of change of the inducing primary field needs to be higher (higher frequency) for materials with lower conductivity. We call the component of the eddy current synchronized with the primary field the in-phase component and the component that is 90° out of phase with the primary field the quadrature component.

Three salient features - a linear range, a quadrature peak, and an inductive limit - occur at different frequency ranges for different objects, but always in the same order.³⁰ At low frequencies, the eddy currents flow through the bulk of the object.^{31,32} They are 90° out of phase with the primary magnetic field, and have magnitude that grows proportionally to the frequency of the magnetic field. In the linear range, material resistivity limits the magnitude of the secondary field. This



Figure 2: (Left) Mock IEDs designed to typify those found in theater. (Right) The Geophex type sensor deployed at Fort AP Hill IED test lanes.

range is not normally used to characterize UXO targets, but is used for applications such as resistivity estimation of soil. As frequency increases, internal eddy currents become out of phase with the primary field and a quadrature peak develops in the secondary field. The frequency of the quadrature peak is a result of object properties such as size, conductivity, magnetic permeability, and shape. In turn, these properties are linked to signal features central to inversion and classification. IEC materials the size of most UXO exhibit this peak in the HFEMI band of 100 kHz-15 MHz,^{13,14,23} As the frequency of the primary field increases further, the eddy currents move to the surface of the object, and the secondary B field plateaus in the inductive limit (i.e. a reflection of the primary field).

In order to detect eddy currents in objects with lower conductivity than metals, the frequency range of traditional EMI sensors had to be increased. In order to sense the equivalent of 15 MHz in the time domain, a time domain instrument would need to turn off the primary magnetic field within $f_{\max} = \frac{1}{\Delta t}$ (where $\frac{1}{\Delta t}$ is the transience of the primary field turnoff), or $\frac{1}{\Delta t} = 67\text{ns}$, which is currently not feasible.³³ Therefore, we developed a frequency domain instrument that could operate at frequencies up to 15 MHz. A more thorough discussion of the iterations of our HFEMI instrument can be found in.¹⁴ To summarize, we found that we needed to shorten the transmitter and receiver coils in order to avoid wave effects on the coils and the resulting field asymmetry. We have fabricated a hybrid coil system³⁴ to increase the signal-to-noise ratio at low frequencies.

3. RESULTS

Improvised explosive devices continue to be the principal asymmetric threat against dismounted troops in theater. State of the art handheld instruments meant to detect buried threats consist of both low-frequency EMI sensors and GPR sensors. While EMI can detect metals and GPR detects dielectric or conductive heterogeneities, both fail to detect and classify some types of IED constituents. Figure 2 shows some typical mock IEDs similar to those found in conflict zones: zigzag wire pressure plates, wooden plungers, tire pressure plates, and carbon rods. Not pictured is another common type of IED and that is the ammonium nitrate fuel oil (ANFO) IED which is usually accompanied by a wire. Current handheld sensors such as the US Army's Handheld Standoff Mine Detection System (HSTAMIDS) and the Anglo-German Vallon - Cobham VMR3 Minehound do not utilize the frequency spectrum between 50 kHz and 20 MHz (the HFEMI frequency regime), and therefore lack the capability to detect and classify these IED constituents.

Fort AP Hill, under the direction of the Night Vision and Electronic Sensors Directorate, maintains IED test lanes containing IED constituent parts buried at different depths. We took our HFEMI instruments there as a test of sensor's capabilities outside of a laboratory environment (see Figure 2 (right)). We tested the sensor over various targets such as a zigzag wire carbon rod pressure plate IED. Figure 3 shows the results in which the contribution from the carbon rod

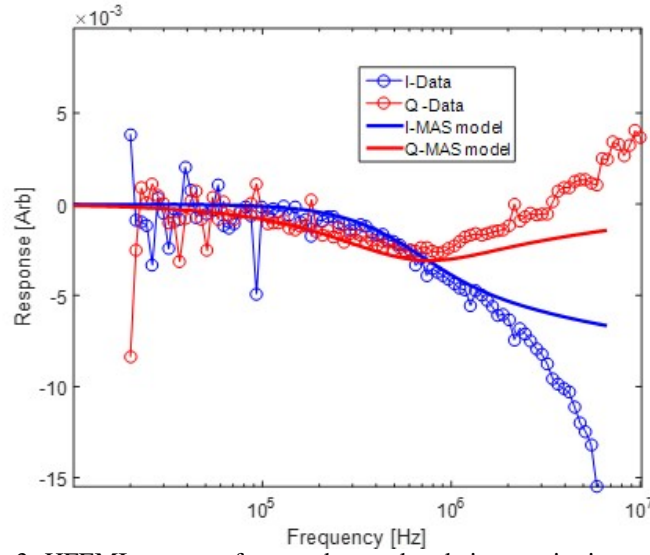


Figure 3: HFEMI response from carbon rod and zigzag wire in a mock IED.

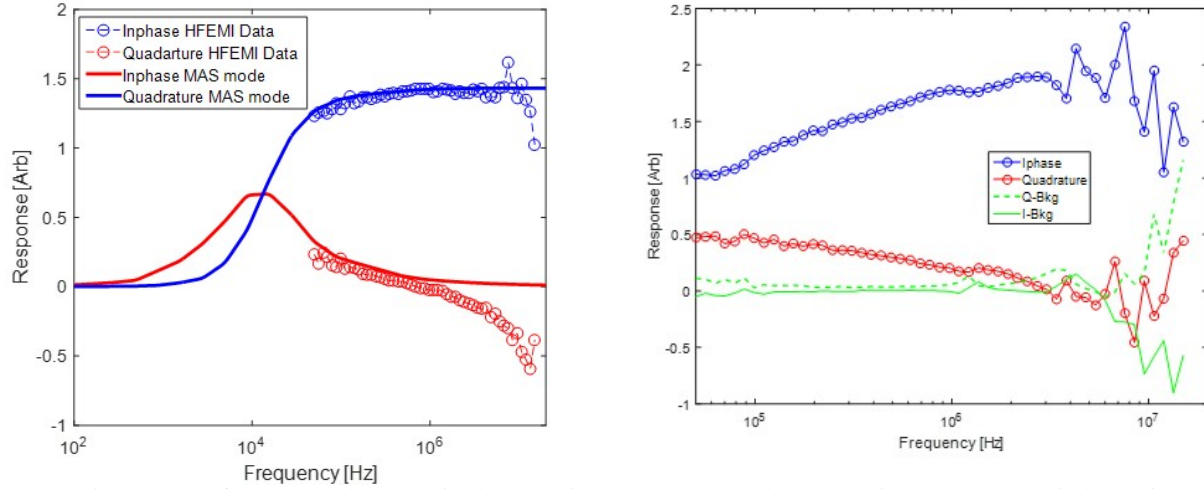


Figure 4: (Left) HFEMI data acquired over a tire type pressure plate, and (right) over a VS-50 landmine.

with a quadrature relaxation peak near one MHz megahertz is clearly identifiable. Also shown are results from the method of auxiliary sources,^{35–39} a numerical model that modeled the carbon rods but not the wires in the pressure plate. The deviation of the data from the model at higher frequencies reflects the presence of the wires in addition to the carbon rods.

We also measured pressure plates made out of tire sections that contain a roughly 3 cm x 5 cm aluminum pressure plate as well as wires leading to the main charge (see Figure 4). With significantly more metal to sustain eddy currents, this pressure plate is easily visible even with low-frequency EMI frequencies. Also shown on the right side of Figure 4 are data acquired over a lower-metal-content landmine, the VS-50 landmine. This landmine has a quarter-sized metallic plate plunge which makes it also easier to identify at lower frequencies, though HFEMI frequencies help with ID in this case.

ANFO IED's are essentially conductivity voids in the soil. As such, normally these would be undetectable by low-frequency EMI sensors, but HFEMI can detect the absence of slightly conductive soils, i.e. a response from the conductivity void in the soil. Figure 5 shows this response as we moved the sensor progressively along the axis of the ANFO IED.

Wires, whether short ($< 1\text{m}$) or longer command wires ($> 1\text{m}$) are not thick enough to sustain sizable eddy currents and therefore are largely undetectable by low-frequency EMI as well as GPR. However Figure 6 shows that both shallow

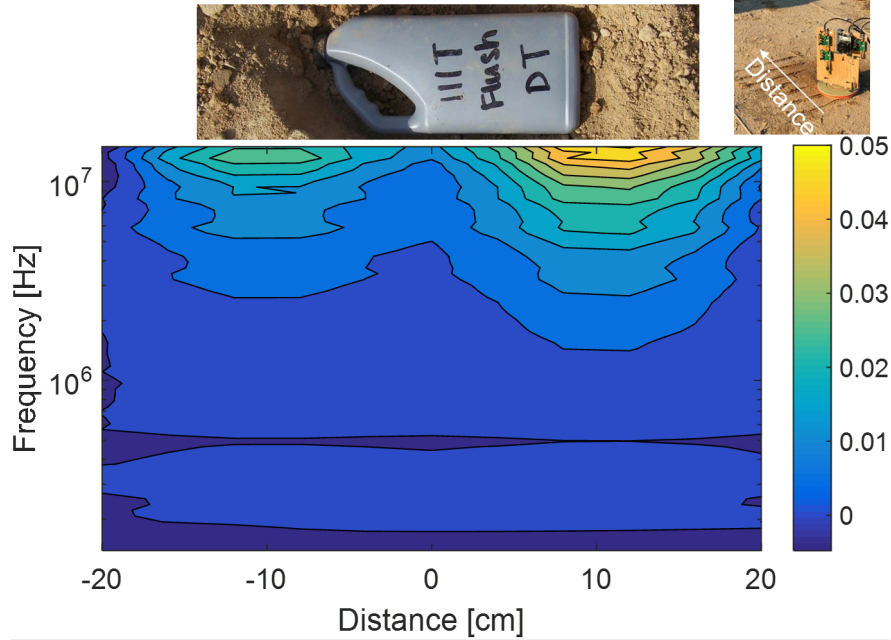


Figure 5: HFEMI inphase response at 10MHz in a line over a jug of ANFO, essentially a conductivity void in the soil.

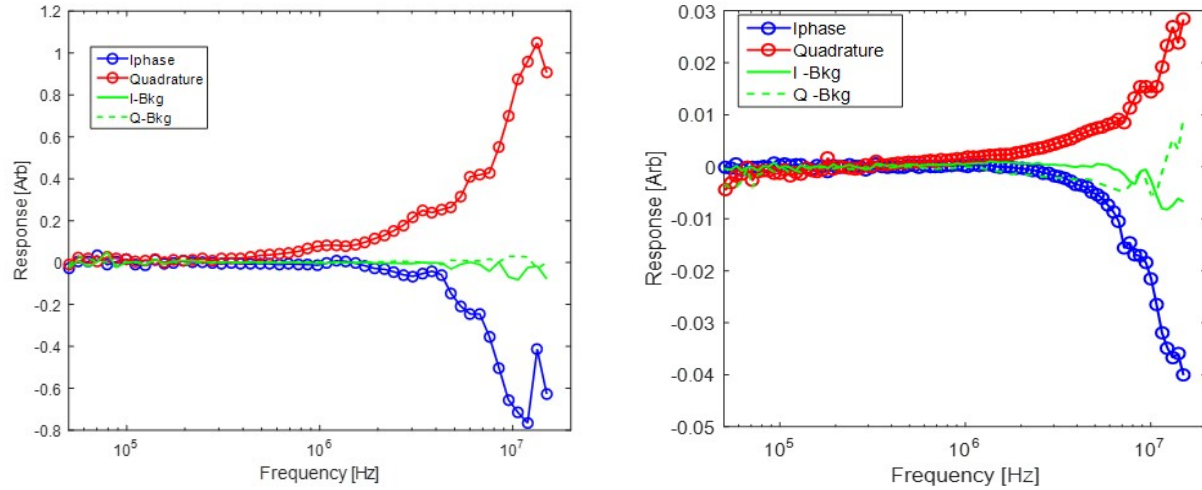


Figure 6: (Left) HFEMI data acquired over a shallow wire ($\approx 1''$ deep), (right) response from similar wire buried at 4'' depth.

and deeper wires are clearly detectable with HFEMI. The range at which these short wires are detectable is greater than the range at which carbon rods, for example, are detectable due to the linear currents set up on the wire that broadcast a magnetic field with a less severe geometrical decay than the more compact carbon rod targets.^{19,20}

4. HFEMI RESULTS OVER TAPWATER AND SOIL

EMI instruments operating under 50 kHz have been used to determine the conductivity of soils for several decades.^{24,40} However, robust standoff measurements of the real part of the soil permittivity remains difficult to acquire at low frequencies as well as at GPR frequencies. In the HFEMI frequency regime, soil permittivity starts to produce a more pronounced effect on the data. We conducted some experiments acquiring HFEMI data over tapwater (≈ 17 mS/m) as well as over Ottawa sand at various stages of saturation. Figure 7 shows results for a broad frequency range and various heights above

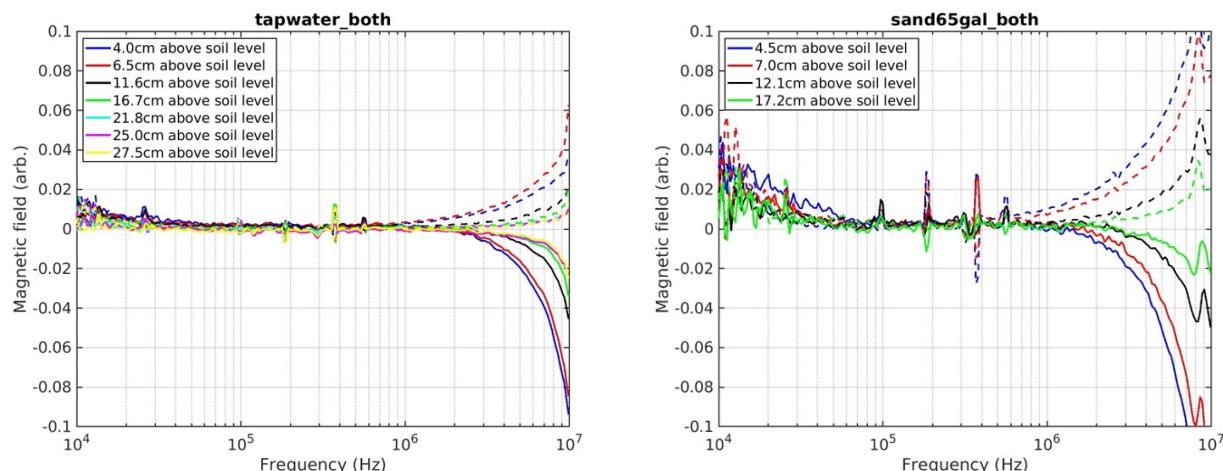


Figure 7: (Left) HFEMI data acquired over an 18 gallon tub filled with tapwater, and (right) data acquired over saturated Ottawa sand 36% VWC as measured by TDR probe.

tapwater on the left and saturated Ottawa sand (36% volumetric water content as measured by a time domain reflectometer) on the right. Potential effects in the HFEMI spectrum due to the presence of the sand can be seen at 7-8 MHz range in Figure 7 (right). This response, noticeable in both the inphase and quadrature responses, is noticeably absent in the results over tapwater alone (Figure 7 (left)).

5. CONCLUSION

Data from the high-frequency electromagnetic induction sensor is providing new insights and via notable responses from classes of less conducting and small targets that have previously remained undetectable by other instruments. Inphase and quadrature relaxation spectra could help identify and detect IED constituent parts such as carbon rods, conductivity voids, short wires, low metallic landmines, and small pressure plates. By reducing the number of turns on the transmitter and receiver coils to avoid wavelength artifacts, EMI spectra in the frequency range of 100 kHz to 20 MHz becomes possible. In this range, new targets become visible, but the soil also becomes a prominent target. Ground effects need to be modeled out or subtracted to identify discrete targets, but those very ground effects can lead to new classes of standoff sensors that ascertain permittivity as well as conductivity. Results from data acquired at the Fort AP Hill IED test lanes suggest that HFEMI could become a viable tool that could be added to existing low frequency EMI instruments in order to better assess and classify threats in theater.

Acknowledgment

This research was sponsored by the US Army ERDC Environmental Quality and Installations UXO program and by the Office of Naval Research (N000141612332).

REFERENCES

1. K. O'Neill, *Discrimination of Subsurface Unexploded Ordnance*, SPIE Press, Bellingham WA, 2016.
2. C. R. Ratto, P. A. Torriane, and L. M. Collins, "Exploiting ground-penetrating radar phenomenology in a context-dependent framework for landmine detection and discrimination," *IEEE Transactions on Geoscience and Remote Sensing* **49**(5), pp. 1689–1700, 2011.
3. I. Shamatava, F. Shubitidze, C. Chen, H. Youn, K. O'Neill, and K. Sun, "Potential benefits of combining EMI and GPR for enhanced UXO discrimination at highly contaminated sites," *Proceedings of SPIE - The International Society for Optical Engineering* **5415**(PART 2), pp. 1201 – 1210, 2004.

4. K. O'Neill, K. Sun, C. Chen, F. Shubitidze, and K. Paulsen, "Combining GPR and EMI Data for Discrimination of Multiple Subsurface Metallic Objects," International Geoscience and Remote Sensing Symposium (IGARSS) **7**, pp. 4157 – 4159, (Toulouse, France), 2003.
5. B. Barrowes, D. Glaser, M. Prishvin, M. Coleman, and F. Shubitidze, "Assessing the frozen state of soils using ifrost: an electromagnetic induction sensor on a uas platform," 18th International Conference on Cold Regions Engineering and the 8th Canadian Permafrost Conference , August 2019. accepted for publication.
6. B. E. Barrowes, J. B. Sigman, K. O'Neill, J. E. Simms, H. J. Bennett, D. E. Yule, and F. Shubitidze, "Detection of conductivity voids and landmines using high frequency electromagnetic induction," Proceedings of International Seminar/Workshop on Direct and Inverse Problems of Electromagnetic and Acoustic Wave Theory, DIPED **2016-December**, pp. 118 – 122, (Tbilisi, Georgia), 2016.
7. J. Hendrickx, B. Borchers, D. Corwin, S. Lesch, A. Hilgendorf, and J. Schlue, "Inversion of soil conductivity profiles from electromagnetic induction measurements," Soil Science Society of America Journal **66**(3), pp. 673–685, 2002.
8. F. Shubitidze, J. P. Fernández, B. Barrowes, I. Shamatava, and K. O'Neill, "Rapid and accurate estimate of the effect of magnetically susceptible soil on MPV-td sensor data using the method of images," XIIIth International Seminar/Workshop on Direct and Inverse Problems of Electromagnetic and Acoustic Wave Theory (DIPED) , Sep. 2008.
9. D. R. Glaser, B. E. Barrowes, M. Prishvin, K. O'Neill, and F. Shubitidze, "Bench scale measurement of unsaturated soils using EMI, IP, TDR, and GPR," Proceedings of the Symposium on the Application of Geophysics to Environmental and Engineering Problems , March 2019. Portlan, OR.
10. B. E. Barrowes, J. P. Fernandez, K. O'Neill, I. Shamatava, and F. Shubitidze, "Electromagnetic induction tools for discrimination of unexploded ordnance: From basic physics to blind tests," FastTIMES **20**, March 2015.
11. SERDP, "Classification applied to munitions response," 2016. <https://www.serdp-estcp.org/Featured-Initiatives/Munitions-Response-Initiatives/Classification-Applied-to-Munitions-Response>.
12. F. Shubitidze, B. Barrowes, J. Sigman, Y. Wang, I. Shamatava, and K. O'Neill, "Detecting and classifying small and deep targets using improved emi hardware and data processing approach," Proceedings of SPIE - The International Society for Optical Engineering **9072**, pp. The Society of Photo–Optical Instrumentation Engineers (SPIE) –, (Baltimore, MD, United states), 2014.
13. J. B. Sigman, B. Barrowes, K. O'Neill, J. Simms, J. Bennett, D. Yule, and F. Shubitidze, "High-frequency electromagnetic induction sensing of non-metallic materials," IEEE Trans. on Geoscience and Remote Sensing **55**(9), 2017.
14. J. E. Simms, J. B. Sigman, B. E. Barrowes, H. H. B. Jr., D. E. Yule, K. O'Neill, and F. Shubitidze, "Initial development of a high-frequency emi sensor for detection of subsurface intermediate electrically conductive (IEC) targets," Journal of Environmental & Engineering Geophysics - Near Surface Geophysical Letters , accepted for publication 2017.
15. B. E. Barrowes, "Patent for - high frequency electromagnetic induction," **14661779**(10001579), 2018/06/19.
16. F. Shubitidze, B. E. Barrowes, J. Ballard, R. Unz, A. Randle, S. L. Larson, and K. A. O'Neill, "High frequency emi sensing for estimating depleted uranium radiation levels in soil," Proceedings of SPIE - The International Society for Optical Engineering **10628**, pp. The Society of Photo–Optical Instrumentation Engineers (SPIE) –, (Orlando, FL, United states), 2018.
17. F. Shubitidze, B. E. Barrowes, J. B. Sigman, and K. O'Neill, "Ultra-wide-band emi sensing for subsurface depleted uranium detection," in Detection and Sensing of Mines, Explosive Objects, and Obscured Targets XXII, Proceedings of SPIE, (Bellingham, WA), Apr. 2017.
18. B. E. Barrowes, F. Shubitidze, J. B. Sigman, J. Bennett, J. E. Simms, D. Yule, and K. O'Neill, "Void and landmine detection using the hfemi sensor," in Detection and Sensing of Mines, Explosive Objects, and Obscured Targets XXII, Proceedings of SPIE, (Bellingham, WA), Apr. 2017.
19. B. E. Barrowes, K. O'Neill, and F. Shubitidze, "High frequency electromagnetic response from short and long wires for ied and tunnel detection," SAGEEP , 2018. Nashville, TN.
20. B. Barrowes, D. R. Glaser, M. Prishvin, K. O'Neill, and F. Shubitidze, "Short and long wire detection using high-frequency electromagnetic induction techniques," Proceedings of SPIE - The International Society for Optical Engineering **10628**, pp. The Society of Photo–Optical Instrumentation Engineers (SPIE) –, (Orlando, FL, United states), 2018.

21. F. Shubitidze, J. Sigman, K. O'Neill, I. Shamatava, and B. Barrowes, "High frequency electromagnetic induction sensing for non-metallic ordnances detection," Proceedings of International Seminar/Workshop on Direct and Inverse Problems of Electromagnetic and Acoustic Wave Theory, DIPED , pp. 180 – 182, (Tbilisi, Georgia), 2014.
22. O. M. Michael Yon, "Low metal content," 2019. <https://www.michaelyon-online.com/low-metal-content.htm>.
23. B. E. Barrowes, J. B. Sigman, Y. Wang, K. A. O'Neill, F. Shubitidze, J. Simms, H. J. Bennett, and D. E. Yule, "Carbon fiber and void detection using high-frequency electromagnetic induction techniques," Proc. SPIE **9823**, pp. 98230D–98230D–10, 2016.
24. B. Barrowes and T. Douglas, "Evaluation of electromagnetic induction (emi) resistivity technologies for assessing permafrost geomorphologies," tech. rep., ERDC - Cold Regions Research and Engineering Laboratory, 2016.
25. D. C. Stewart, W. L. Anderson, T. P. Grover, and V. F. Labson, "Shallow subsurface mapping by electromagnetic sounding in the 300 khz to 30 mhz range: Model studies and prototype system assessment," Geophysics **59**(8), pp. 1201–1210, 1994.
26. D. Stewart, W. Anderson, T. Grover, , and V. Labson, "A new instrument and inversion program for near-surface mapping - high frequency em sounding in the frequency range of 300 khz-30mhz," in Proceedings of 60th Annual Meeting: Society of Exploration Geophysicists **60**, p. 130, 1990.
27. H. Huang and D. C. Fraser, "Dielectric permittivity and resistivity mapping using high-frequency, helicopter-borne em data," Geophysics **67**(3), pp. 727–738, 2002.
28. G. Olhoeft and D. Strangway, "Magnetic relaxation and the electromagnetic response parameter," Geophysics **39**(3), pp. 302–311, 1974.
29. D. K. Cheng, Field and Wave Electromagnetics, vol. 2, Addison-Wesley, New York, 1989.
30. F. S. Grant and G. F. West, Interpretation Theory in Applied Geophysics, McGraw-Hill, New York, 1965.
31. F. Shubitidze, J. P. Fernandez, B. E. Barrowes, I. Shamatava, A. Bijamov, K. O'Neill, and D. Karkashadze, "The orthonormalized volume magnetic source model for discrimination of unexploded ordnance," IEEE Transactions on Geoscience and Remote Sensing **52**(8), pp. 4658 – 4670, 2014.
32. J. R. Wait, Geo-Electromagnetism, New York: Academic Press, 1982.
33. C. Nelson, C. Cooperman, W. Schneider, D. Wenstrand, and D. Smith, "Wide bandwidth time-domain electromagnetic sensor for metal target classification," IEEE Transactions on Geoscience and Remote Sensing **39**(6), pp. 1129–1138, 2001.
34. J. B. Sigman, B. E. Barrowes, Y. Wang, H. J. Bennett, J. E. Simms, D. E. Yule, K. O'Neill, and F. Shubitidze, "Coil design considerations for a high-frequency electromagnetic induction sensing instrument," Proceedings of SPIE - The International Society for Optical Engineering , 2017.
35. F. G. Bogdanov, D. D. Karkashadze, and R. S. Zaridze, "The method of auxiliary sources in electromagnetic scattering problems," Generalized multipole techniques for electromagnetic and light scattering: Elsevier Science , 1999.
36. F. Shubitidze, J. P. Fernández, B. E. Barrowes, I. Shamatava, and K. O'Neill, "The method of auxiliary sources for solving low-frequency electromagnetic induction problems in underwater environments," in Applied Computational Electromagnetics Symposium (ACES), (Williamsburg, VA), Mar. 2011.
37. F. Shubitidze, K. O'Neill, S. A. Haider, K. Sun, and K. D. Paulsen, "Application of the method of auxiliary sources to the wide-band electromagnetic induction problem," IEEE Trans. on Geosci. Remote Sens. **40**, pp. 928–942, April 2002.
38. F. Shubitidze, K. O'Neill, I. Shamatava, K. Sun, and K. Paulsen, "Analysis of geological soil effects on EMI responses relevant to UXO discrimination," Proceedings of SPIE - The International Society for Optical Engineering **5794**(PART I), pp. 296 – 307, 2005.
39. F. Shubitidze, K. O'Neill, S. Haider, K. Sun, and K. Paulsen, "Analysis of induction responses from metal objects using the method of auxiliary sources," Conference Proceedings 2000 International Conference on Mathematical Methods in Electromagnetic Theory (Cat. No.00EX413) **2**, pp. 468 – 70, 2000.
40. Y. Das, "Effects of soil electromagnetic properties on metal detectors," IEEE Trans. Geosci. Remote Sensing **44**, pp. 1444–1453, June 2006.